Optimizing a Rotating Tilt Sensor for the LISA Torsion Pendulum

Eric Raymer
Eöt-Wash Group
CENPA
University of Washington
Physics REU, Summer 2006

1. Abstract

The Eöt-Wash group at the University of Washington has developed a torsion pendulum to investigate noise sources in the Laser Interferometer Space Antenna (LISA) caused by small forces acting on its test masses. To ensure a high amount of accuracy in the torsion pendulum's measurements, the platform upon which the pendulum rests must remain as level as possible. The use of a rotating tilt sensor provides an effective way to measure the tilt present in the system while eliminating the adverse effects of zero-point drift. In this paper, we discuss improvements made to both the hardware and the software of the rotating tilt sensor. The result of the improvements is a tilt sensor that is primarily hardware controlled, and is capable of higher rotation frequencies as well as integrated data analysis.

2. Background

2.1 Gravitational Waves

Einstein's general theory of relativity describes spacetime as dynamic rather than the static backdrop of classical physics. The presence of mass causes spacetime to curve, and this curvature is what produces the force we know as gravity. Einstein's equations predict that the acceleration of a quadrupole mass moment will produce propagating "ripples" in spacetime. These "ripples," which are time-varying oscillations of spacetime, are known as gravitational waves.

Any accelerating mass with a quadrupole moment will produce a gravitational wave, but in most cases the magnitude of the waves are far too small to be detected. The amplitude of the waves decreases with distance, so that in many cases gravitational waves from distant sources will be imperceptible. An observable gravitational wave requires the acceleration of extremely massive objects. Some examples of systems that may produce detectable gravity waves are coalescing binary stars (Figure 1), a star being "eaten" by a black hole, and the merging of two black holes.

Figure 1: Gravitational waves produced by a binary system.

While gravitational waves have not yet been observed directly, gravitational wave detection is a topic of interest for a number of reasons. In addition to providing another verification of general relativity, being able to detect gravitational waves would open up a new window of observation of the universe. The frequencies of gravitational waves that are expected to be observable are much lower than those of observed astronomical electromagnetic radiation, and can reveal details about the bulk motion of dense energy concentrations in the universe. Information about the early universe could also be uncovered by examining the low frequency stochastic gravitational wave background – this is analogous to the cosmic microwave background created as a result of the big bang.

2.2 Gravitational Wave Detection using LISA

The presence of a gravitational wave will cause the distance between two objects to increase and decrease at the frequency of the gravitational wave as the wave stretches and compresses the space the object inhabits. This principle underlies the method of gravitational wave detection using laser interferometry. If a gravitational wave passes through a laser interferometer, the lengths of the interferometer arms will change, resulting in a change in the phase difference of the recombined light. This varying phase difference can be detected by a photodiode as a variation in intensity, which can then be related to the gravitational wave strain - a measure of the "strength" of the gravitational wave.

Figure 2: A cutaway view of a LISA spacecraft. Each spacecraft contains two test masses.

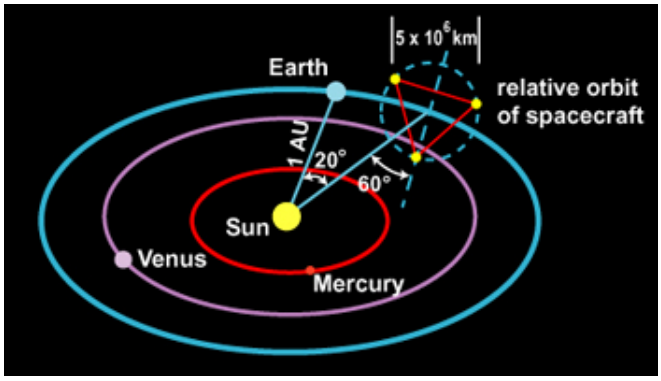

Figure 3: The orbits of the LISA spacecraft.

The Laser Interferometer Space Antenna (LISA) consists of three spacecraft (Figure 2) that will orbit the sun in an equilateral triangle with sides five million kilometers long (Figure 3). The orbit of the each individual spacecraft will be slightly elliptical, so that the triangle formation can be maintained as the arrangement orbits the sun. Each spacecraft will act as an interferometer, using the other two as arms. This arrangement will orbit the sun twenty degrees behind the earth, to minimize the adverse effects of the earth and sun's gravitational fields. Polished test masses (Figure 4) will float freely within each spacecraft and reflect the incoming lasers. When a gravitational wave passes through the apparatus, the distances between test masses will shift slightly, and result in a measurable change in phase difference between the interfering laser light.

The motion of the test masses will be on the order of 10 picometers – about one tenth the size of an atom.

Because they are sensitive to motion on these incredibly small scales, it is imperative that the test masses in LISA experience no forces other than that of gravity. Forces such as those from the solar wind, radiation pressure, and the solar magnetic field can be negated by the shielding of the spacecraft and through small thrusters used to correct the motion of the spacecraft. However, a number of internal forces arise due to the small distances (2-4 mm) between the test masses and their housings. Outgassing, which arises due to temperature fluctuations within the test mass chamber, may cause gas bubbles trapped in the test mass or housing to escape, and as they propel themselves away, cause a force in the opposite direction. Patch effects may also arise due to differences in the work functions between two different metals that are in close proximity. Electrons will flow from one metal to another due to the difference in the two metals' work functions, resulting in a buildup of charge that leads to electrostatic forces. There is also some small gravitational coupling between the test mass and the spacecraft itself.

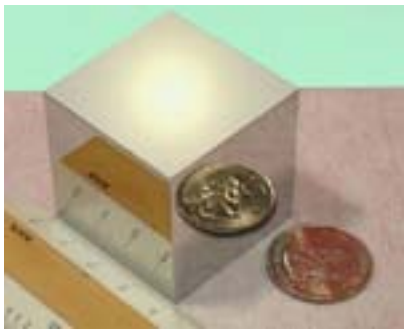

Figure 4: A LISA test mass (placed next to a quarter to show its scale).

2.3 The LISA Torsion Pendulum

The University of Washington's Eöt-Wash group has developed a torsion pendulum (Figure 5) to emulate the forces that the LISA test masses will experience. This apparatus will allow a greater understanding of the noise sources produced by these small forces. The torsion pendulum consists of a plate that hangs from a tungsten fiber. The plate hangs a small distance away (2-4mm) from another test plate. These test plates mimic the test mass and housing on the LISA spacecraft. The forces between these two plates will produce a measurable torque on the pendulum. It is critical that there is no change in the tilt of the apparatus, as a varying tilt will produce unwanted noise in the measurements.

A rotating tilt sensor is part of a feedback system that will help to ensure that the apparatus is entirely level. A rotating sensor has the advantage of eliminating zero-point drift that is present in stationary sensors. Zero-point drift is a small variation in the output, and is independent of the actual tilt. For example, if the tilt sensor is entirely level, the output will not be constant, but will vary with time. This variation is the zero-point drift. Rotating the sensor will

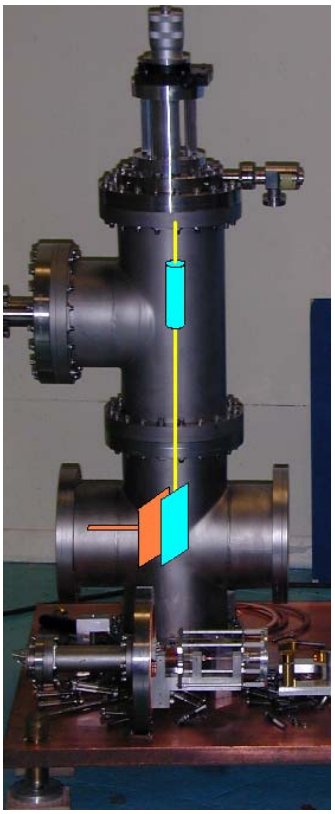

Figure 5: The LISA Torsion Pendulum

produce a oscillating signal that we can fit to a sinusoidal function, $f(t)=z(t) + A(t) \sin(2\pi\omega t\varphi)$. By extracting the coefficient of the sine term, we are able to obtain a measure of the tilt while ignoring the zero-point drift ($z(t)$).

3. Rotating Tilt Sensor

3.1 Hardware

The primary component of the apparatus is an Applied Geomechanics Series 755 Miniature Tilt Sensor. The sensor is a small tube filled with a conducting fluid and a bubble. Three electrodes are immersed inside the fluid. As the tilt sensor tilts, the bubble moves back and forth along the tube, resulting in a change in electrode surface area in contact with the conducting fluid. This change will produce a varying resistance between the electrodes, which will in turn change the voltage across them. This varying output voltage provides a measure of the tilt.

The tilt sensor is located inside a circular box, above which sits a box housing the tilt sensor's electronics (Figure 6). The sensor and electronics are mounted on a shaft that passes through a circular plate. The plate has three "legs" consisting of equally spaced screws, two of which can be adjusted manually to vary the tilt of the plate. These three screws rest atop a cylinder of larger diameter. Inside this cylinder, the main shaft is connected to a brass bellows. The bellows is attached to the stepper motor that drives the tilt sensor.

Figure 6: The rotating tilt sensor.

3.2 Interface and Software

The stepper motor and output signals are controlled by a LabWindows/CVI program that is interfaced with a National Instruments USB-6008 Data Acquisition Device (DAQ). A schematic of the original arrangement is shown in Figure 7.

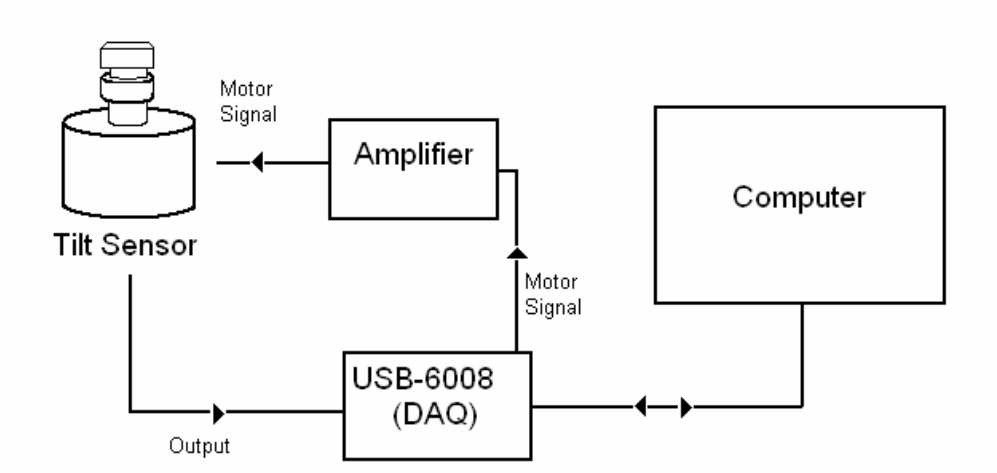

The original software drove the motor by creating a sequence of digital signals that were sent directly to the stepper motor via the digital output port on the DAQ. The timing of the signals was software controlled. A stream of data was recorded at a constant rate. The program recorded four numerical values for the following variables: positive tilt, negative tilt, temperature, and a zero-mark indicator. As they were recorded, these values were displayed graphically on a strip chart, and as numerically values on a display panel.

3.3 Desired Improvements

A number of improvements were made to both the tilt sensor hardware and the software program. All improvements were made with two goals in mind: first, that the tilt sensor would be able to rotate at a higher frequency, and second, that the software would be adjusted to provide a more stable method of data collection and analysis. A higher rotation frequency provides quicker feedback about the current tilt of a system. The software-controlled motor and data collection methods were functional, but not reliable, especially when running the motor at a high frequency. Other software processes running simultaneously with the tilt sensor interface can consume the system's resources and produce unnecessary delays in the motor speed and/or data collection. It was necessary to have a stable method of data collection that did not depend mainly on the system used to run the software.

4. Improvements to the Tilt Sensor

4.1 Stepper Motor

A new stepper motor was installed on the tilt sensor so as to achieve higher rotation frequencies. The motor we used moved 1.8 degrees per step, for a total of 200 steps per revolution in full mode (or 400 steps per revolution in half-step mode). We desired a rotation frequency of approximately 0.1 Hz, which requires a stepping frequency of at least 20 Hz (or 40 Hz in half-step mode).

4.2 New Circuit Elements

To relieve the computer of the responsibilities of driving the motor and continuously collecting data, we implemented a number of new software controlled

circuit elements, each of which handled different aspects of the tilt sensor. These elements were integrated into a motor controller circuit, which handled the responsibilities of both data collection triggering and driving the motor. The figure below is a schematic of the new tilt sensor design.

4.2.1 Motor Controller

To control the stepper motor, we created a circuit utilizing the SGS-Thomson Microelectrics L297 Stepper Motor Controller and L298 Dual Full Bridge Driver chips. The L297 accepts digital signals from the software program and produces an output driving signal. One of the required input signals is a clock timer, which controls the stepping rate of the motor. The other inputs enable the motor to start or stop, and control the motor's half/full step mode and the direction of rotation. The TTL signals produced by the L297 are passed on to the L298, which amplifies the signal so that it can be used to drive the motor.

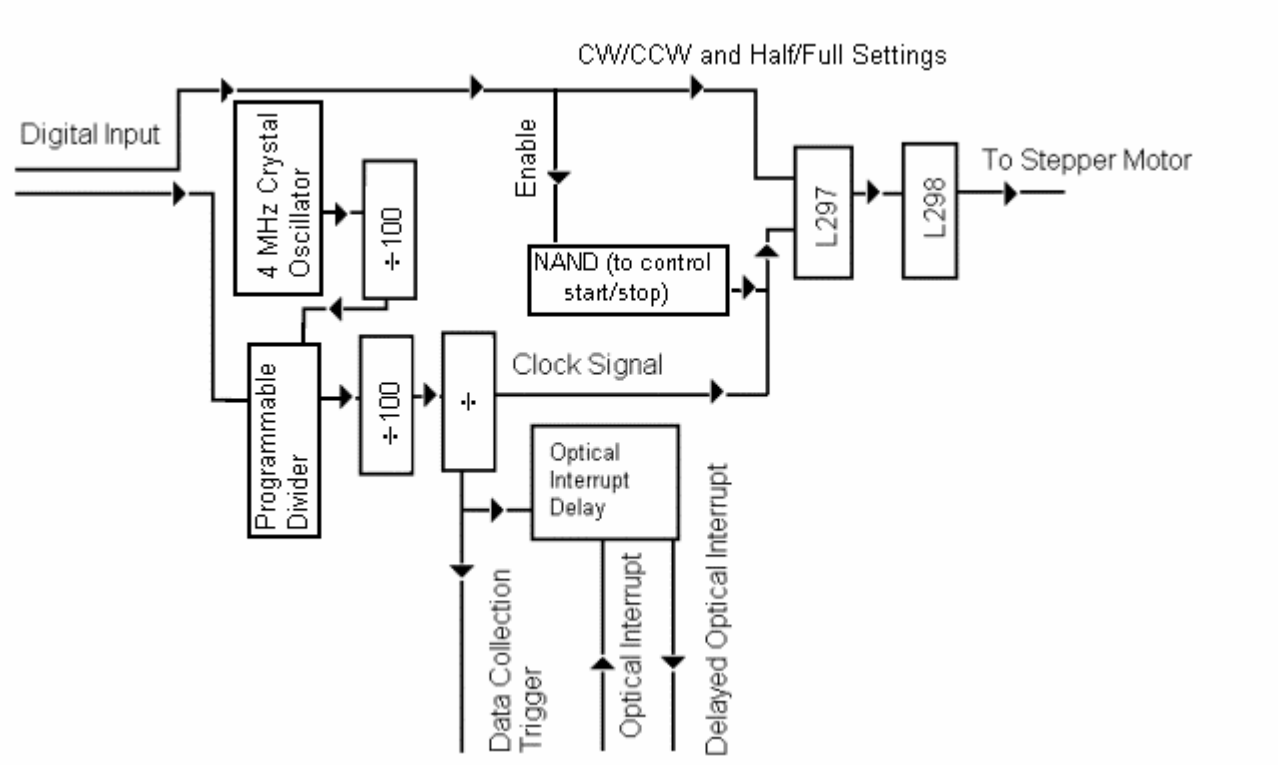

Figure 8: Details of the motor controller circuit.

4.2.2 Crystal Oscillator

There were a number of options available for the clock timer required to drive the stepper motor. As mentioned previously, the software driven timing scheme was very unstable, so we attempted to find a hardware based solution that would produce more acceptable results. We desired a timer that would operate at an exceptionally stable frequency, and the SG-51 Crystal Oscillator chip was a suitable choice. The crystal oscillator produces a stable 4 MHz signal, which was fed into several 74HC390 dual

decade ripple counters connected in series. The 74HC390 chips allowed us to divide the frequency down to the rate that we desired for our clock signal. The signal from the 74HC390 chips was then passed on to a 74LS193 Presettable 4-bit Binary Up/Down Counter. We controlled this counter using a digital output signal generated by the software. By varying the number of counts the 74LS193 waited before producing a signal, it is possible to control how much the frequency is divided. This allows us to control the clock timer (and thus the rotation frequency) through controls on the user interface. The rotation frequencies we are able to attain range from 0.25 Hz (for a 50 Hz stepping frequency in full-step mod) to 0.0715 Hz (for a 28.6 Hz stepping frequency in half-step mode).

4.2.3 Optical Interrupt

During the data analysis runs, we wish to keep track of when a full rotation of the tilt sensor has occurred. To record this, an optical interrupt switch was mounted on the inside of the large cylinder of the tilt sensor. The optical interrupt consists of two small arms (Figure 9), one of which shines a small infrared beam onto a sensor located on the other arm. When this beam is blocked, the interrupt will output a positive voltage signal until the beam is broken, after which the signal drops back to a low voltage. We placed the optical interrupt so that a disk attached to the main shaft blocked the infrared beam. A thin slot was cut into the disk so that the optical interrupt would be triggered once every full revolution. By measuring only the rising or falling edge of the interrupt signal, the width of the slot became inconsequential.

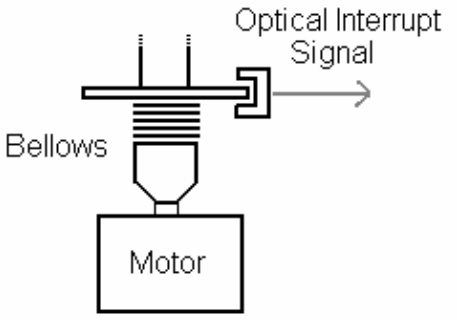

Figure 9: The optical interrupt placed around the bellows.

4.2.4 Timing Concerns

The crystal oscillator is used as a timer to drive the motor and also as a trigger for data collection. It was unnecessary (and potentially too demanding upon the computer) to take data continuously. By dividing the motor signal by a factor of ten, we were able to obtain another signal that could be used to trigger data collection at a rate of one sample for every ten steps of the motor.

The zero-mark signal only occurs during one step per revolution, and since data is sampled every ten steps, it was likely that the zero-mark signal would only occasionally appear in the recorded data. So that the zero-mark would not be missed during the data collection, a small digital logic circuit was installed to process the zero-mark signal. This circuit acts as a flip-flop, and simply delays the falling edge of the zero-mark. When the zero-mark occurs, the output is maintained at a high voltage until receiving a signal from the clock that triggers data collection. At the falling edge of the clock signal, the output is reset to low until the zero-mark occurs again. This delay allowed us to ensure that we would not miss any zero-mark signals.

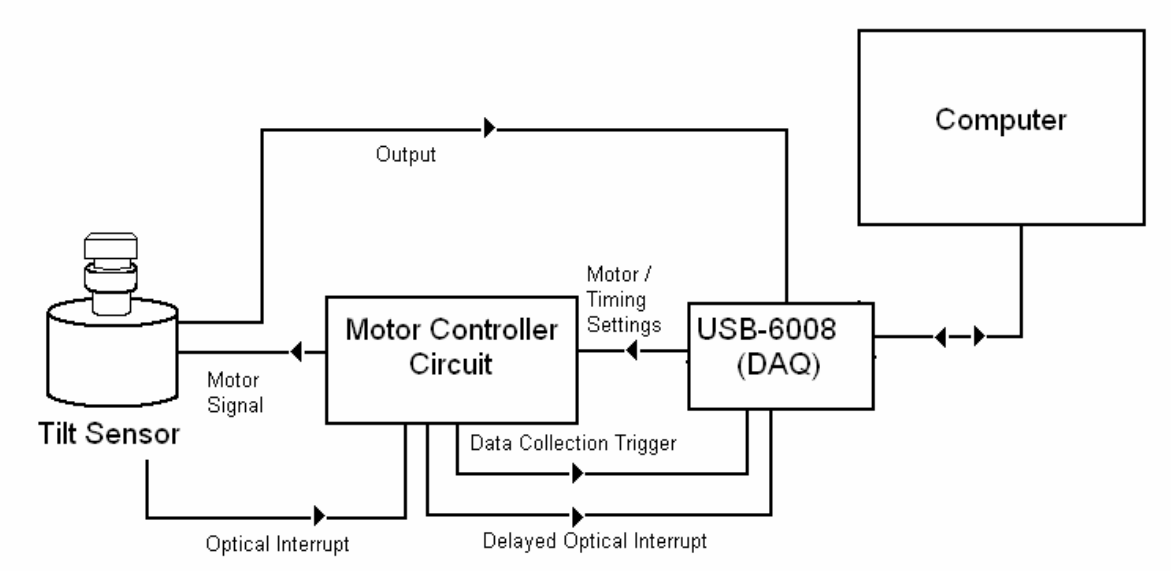

Figure 10: The new tilt sensor setup.

4.3 Software Improvements

The implementation of new hardware required the development of software that could control the new components. A number of user interface controls were modified, and some new features were added. In addition, we also desired that data analysis routines be implemented within the program, so that the amount of analysis required by the user would be decreased.

4.3.1 User Interface Controls

The appearance of the user interface was left mostly intact, but the "machinery" behind the controls required modification to accommodate the new hardware. Also, two new buttons were added: one that would stop the motor when a zero-mark signal occurred and another that would rotate the motor by 90 degrees. These controls were designed to assist data collection for runs in which the motor remained stationary.

4.3.2 Data Analysis Software

The DAQ continuously samples data, and the program collects this data from the DAQ's buffer periodically. The program sifts through the collected data points and looks for the peak on the data collection clock. When a high peak occurs, the program stores the data points that occurred simultaneously with that peak. These raw data points are printed into a file.

During data collection, the program monitors how many zero-marks have occurred since the data run began. Each zero-mark indicates the beginning of a new period of the tilt signal. The program will perform data analysis after a user-specified

number of periods have taken place. Each block of data is fitted to a sinusoidal function of the form $f(t) = o + \sum_n a_n \cos(\omega_n t) + b_n \sin(\omega_n t)$. The data is fitted over n different frequencies that are specified within the program. The analysis software extracts the offset o, as well as the coefficients, a_n and b_n. These sine and cosine coefficients give the x and y components of the tilt. All of the coefficients are written to an output file.

5. Results

Numerous test runs were performed with the tilt sensor so that we could analyze its performance. On these runs, the screws on the tilt sensor's plate were adjusted so that the tilt of the system was minimized. Data was collected overnight. Using the Fast Fourier Transform algorithm allowed us to obtain a power spectrum from the raw tilt data. From this spectrum we were able to identify the frequencies at which the largest amplitude components of the output occurred. A sample power spectrum is shown in Figure 11. Note that the largest peak occurs at the rotation frequency.

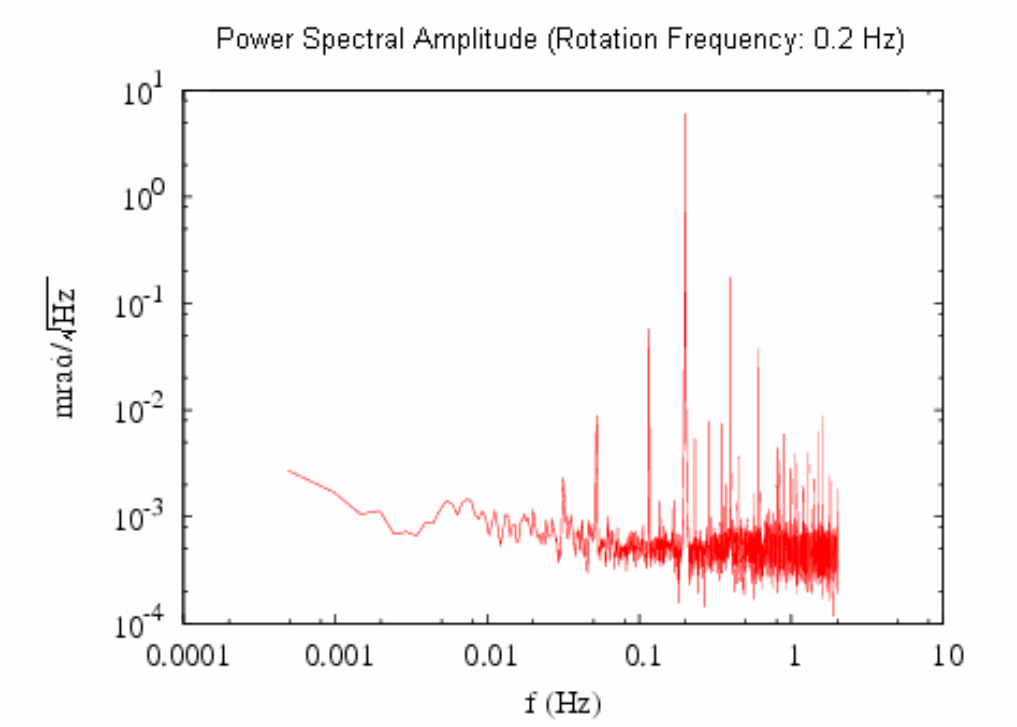

Figure 11: A plot of power spectral amplitude for a rotation frequency of 0.2 Hz.

We set the data analysis code to fit the raw data to a sum of sinusoidal functions with frequencies equal to the rotation frequency, and the two frequencies with the next largest amplitudes. The coefficients of the sine and cosine terms that were fit to the rotation frequency represent the tilt along the x and y axes of the sensor. Figure 12 shows the power spectral amplitude of the tilt along one axis for both rotating and stationary data runs. For low frequencies, the noise present in the rotating sensor is lower than that of the stationary sensor. However, for higher frequencies, the noise in the stationary

sensor is lower. Note that for the data from the rotating sensor there are two frequencies with large amplitude components that were not fit by the data analysis routines.

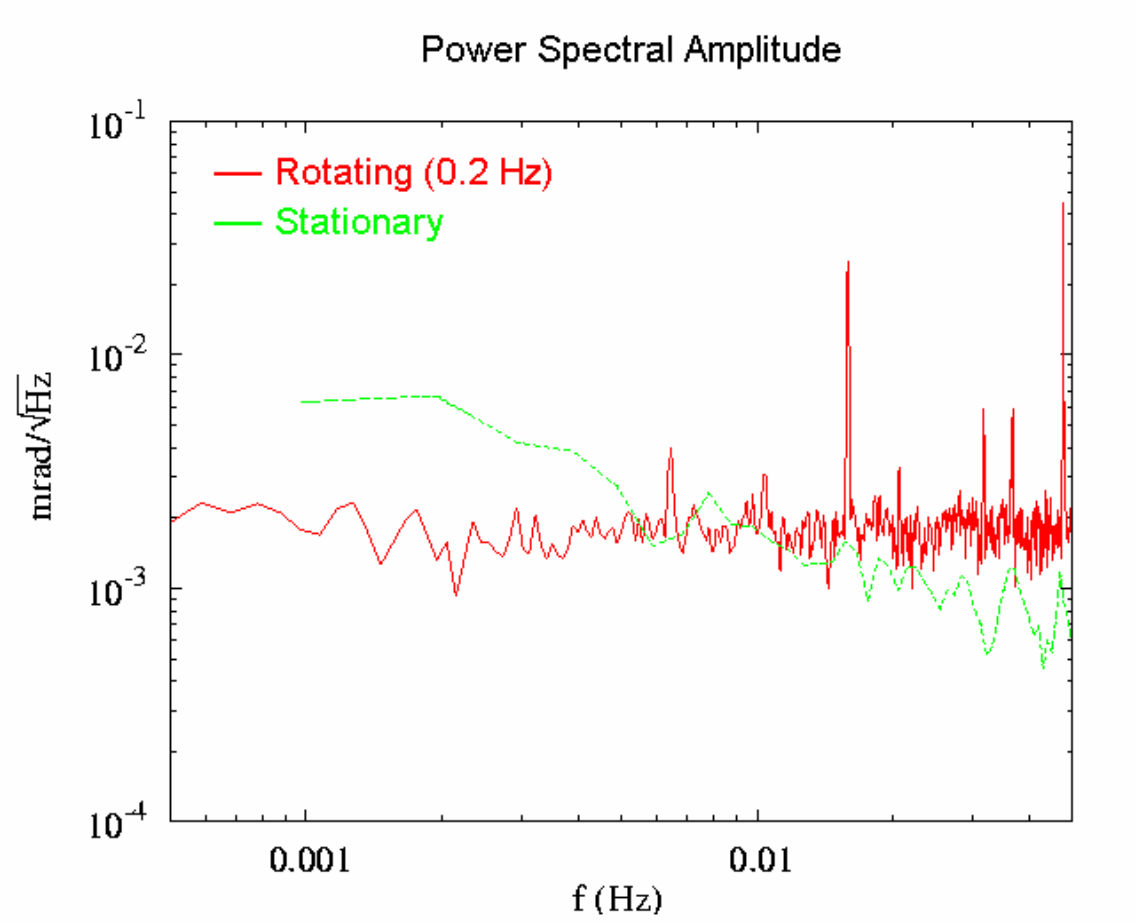

Figure 12: Power spectral amplitude of the tilt for the rotating sensor (0.2 Hz) and the stationary sensor.

6. Conclusion

The modifications to the rotating tilt sensor were made with two goals in mind: to increase the rotation frequency, and to provide a more stable method of data collection. Both goals were met. The tilt sensor is now capable of reliably attaining speeds greater than 0.1 Hz. The new hardware provides a stable method of driving the motor and the software is now capable of performing inline data analysis. For low frequencies, the rotating sensor has a significantly lower noise level than the stationary sensor.

7. Acknowledgements

I would like to thank the Eöt-Wash group for allowing me to work with them this summer. In particular, I would like to thank my advisor, Blayne Heckel, as well as Stephan Schlamminger and Erik Swanson for all of their assistance and guidance throughout the REU program. This project would not have been possible without their support. I would also like to thank David Hyde for his help in the machine shop. Finally, I would like to thank the National Science Foundation and the University of Washington for hosting the REU program.

8. References

- Chaurasiya, Kathy. *Rotating Tilt Sensor for LISA Torsion Pendulum.* REU Paper, http://www.int.washington.edu/REU/2005/Kathy_paper.pdf. 2005.
- Goodenough, Lisa. *$1/f^{\alpha}$ Noise Outwitted – A Rotating Tilt Sensor.* M.S. Thesis, University of Washington. 2005.
- Heckel, Blayne. Private Communication.
- Laser Interferometer Space Antenna. http://lisa.jpl.nasa.gov.
- Schlamminger, Stephan. Private Communication.
- Sigg, Daniel. *Gravitational Waves.* http://www.ligo-wa.caltech.edu/ligo_science/P980007-00.pdf. 1998
- Thorne, Kip S. *Gravitational Waves.* ArXiv:gr-qc/9506086. 1995.